Inorganic Chemistry

Article

pubs.acs.org/IC

2,6-Bis(5-(2,2-dimethylpropyl)-1*H*-pyrazol-3-yl)pyridine as a Ligand for Efficient Actinide(III)/Lanthanide(III) Separation

Antje Bremer, [†,‡] Christian M. Ruff, [†,‡] Denise Girnt,[§] Udo Müllich, [†] Jörg Rothe, [†] Peter W. Roesky,*[,§] Petra J. Panak,*[,†,‡] Alexei Karpov,[∥,⊥] Thomas J. J. Müller,[∥] Melissa A. Denecke, [†] and Andreas Geist*[,†]

[†]Institut für Nukleare Entsorgung, Karlsruher Institut für Technologie (KIT), P.O. Box 3640, 76021 Karlsruhe, Germany

[‡]Institut für Physikalische Chemie, Ruprecht-Karls-Universität Heidelberg, Im Neuenheimer Feld 234, 69120 Heidelberg, Germany

[§]Institut für Anorganische Chemie, Karlsruher Institut für Technologie (KIT), Engesserstraße 15, 76131 Karlsruhe, Germany

[∥]Institut für Organische Chemie und Makromolekulare Chemie, Heinrich-Heine-Universität Düsseldorf, Universitätsstraße 1, 40225 Düsseldorf, Germany

Supporting Information

ABSTRACT: The N-donor complexing ligand 2,6-bis(5-(2,2-dimethylpropyl)-1*H*-pyrazol-3-yl)pyridine (C5-BPP) was synthesized and screened as an extracting agent selective for trivalent actinide cations over lanthanides. C5-BPP extracts Am(III) from up to 1 mol/L HNO_3 with a separation factor over Eu(III) of approximately 100. Due to its good performance as an extracting agent, the complexation of trivalent actinides and lanthanides with C5-BPP was studied. The solid-state compounds $[Ln(C5\text{-}BPP)(NO_3)_3(DMF)]$ (Ln = Sm(III), Eu(III)) were synthesized, fully characterized, and compared to the solution structure of the Am(III) 1:1 complex $[Am(C5\text{-}BPP)(NO_3)_3]$. The high stability constant of log β_3 = 14.8 ± 0.4 determined for the Cm(III) 1:3 complex is in line with C5-BPP's high distribution ratios for Am(III) observed in extraction experiments.

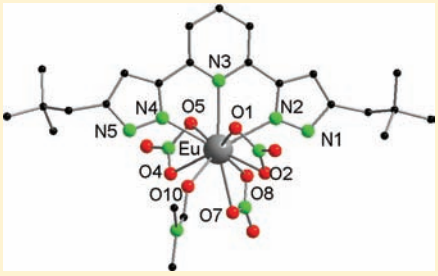

INTRODUCTION

Chemical liquid−liquid extraction is a widely and successfully applied technique for separating ionic solutes. However, customary extracting agents which coordinate metal ions via oxygen donor atoms are not useful for separating trivalent actinide and lanthanide ions, due to the similar chemistry of these elements. Their separation is an essential part of innovative nuclear fuel cycles, which are under development in many countries.[1−3]

Nitrogen heterocycle compounds such as terpyridine derivatives form stronger complexes with trivalent actinides than with lanthanides, initiating the search for new N-donor extracting agents.[4,5] Unfortunately, most of these compounds do not work in solutions of relatively high nitric acid concentrations (0.5 mol/L and greater), which is a process requirement. Alkylated 2,6-ditriazinylpyridines (BTP),[6−8] alkylated 6,6′-ditriazinylbipyridines (BTBP),[9−11] and their phenanthroline derivates (BTPhen)[12] have been developed (Scheme 1) and are able to directly extract trivalent actinides from nitric acid solutions with high selectivity over the lanthanides. Typically, separation factors for Am(III) over Eu(III) (as representatives of trivalent actinides and lanthanides) of 100−300 are achieved.

Despite huge progress being made, all of the known N-donor extracting agents have some unfavorable properties, and the search for even better compounds continues.

Recent efforts are directed not solely at synthesizing new N-donor extracting agents and testing them for selective extraction of trivalent actinides but also at studying them from a more fundamental point of view; this is true for BTP and BTBP in particular.[13−29] The goal of such fundamental studies is understanding their selectivity on a molecular level, which in turn could have a positive impact on the development of new compounds with improved properties.

Following the approach of slightly modifying the BTP skeleton, we synthesized 2,6-bis(5-(2,2-dimethylpropyl)-1*H*-pyrazol-3-yl)pyridine (C5-BPP; Scheme 2).[30−33] The structure of C5-BPP can be viewed as intermediate between the BTPs and 6-(3,5-dimethyl-1*H*-pyrazol-1-yl)-2,2′-bipyridine (dmpbipy), a ligand with weak complexing power for the trivalent actinides studied earlier.[34]

In the following, results from liquid−liquid extraction studies for Am(III) and Eu(III) are presented and the solid-state structures of C5-BPP complexes with Sm(III) and Eu(III) are described. These structures are compared to the solution structure of an Am(III) complex characterized by extended X-ray absorption fine structure (EXAFS). Stability constants of the Cm(III) 1:1, 1:2, and 1:3 complexes are determined by time-resolved laser fluorescence spectroscopy (TRLFS) and compared to those for the Cm(III)-BTP[26] and Cm(III)-dmpbipy[34] complexes.

Received: January 10, 2012
Published: April 19, 2012

   dx.doi.org/10.1021/ic3000526 | *Inorg. Chem.* 2012, 51, 5199−5207

Scheme 1. BTP, BTBP, and BTPhen

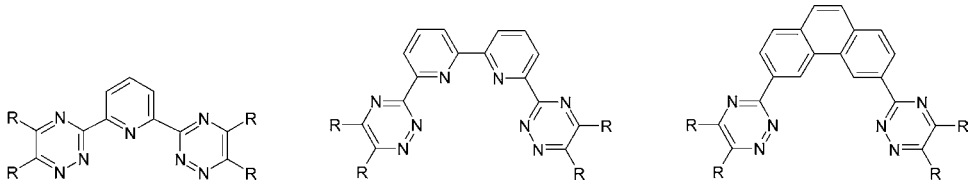

Scheme 2. C5-BPP

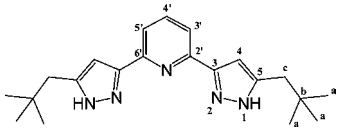

EXPERIMENTAL SECTION

Instrumentation and Measurements. NMR spectra were recorded on a Bruker Avance III 400 MHz or a Bruker Avance II 300 MHz spectrometer. Chemical shifts are referenced to internal solvent resonances and are reported relative to tetramethylsilane (^{1}H NMR). IR spectra were obtained on a Bruker Tensor 37 FT-IR instrument. Mass spectra were recorded at 70 eV on a Varian Mat SM 11 instrument. Elemental analyses were carried out with an Elementar vario EL or vario MICRO cube apparatus. Melting points were measured in open glass capillaries in a Stuart SMP30 melting point apparatus.

TRLFS measurements were performed using a Nd:YAG (Surelite, Continuum) pumped dye laser system (Narrow Scan G-R, Radiant Dyes). A wavelength of 396.6 nm was used for excitation of Cm(III). Emission spectra were recorded in the range of 565−645 nm after a delay time of 1.0 μs to discriminate the Cm emission from the short-lived fluorescence of the organic ligand. The fluorescence emission was detected by a spectrograph (Shamrock 303i, ANDOR) with a 900 lines/mm grating and an ICCD Camera (iStar Gen III, ANDOR). The cuvette holder is temperature controlled; all measurements were performed at T = 20 °C.

Am L3 edge X-ray absorption fine structure (XAFS) spectra were recorded at the INE-Beamline for actinide research at the ANKA synchrotron light source.[35] Higher harmonic radiation in the incident X-ray beam was suppressed by detuning the double crystal monochromator (DCM)—equipped with a pair of Ge ⟨422⟩ crystals—to 70% of maximum photon flux peak intensity. The incident intensity was measured by an Ar-filled ionization chamber at ambient pressure. The Am L3 scans were calibrated against the first inflection point in the X-ray absorption near-edge structure (XANES) spectrum of a Nb foil, defined as 18 986 eV. Spectra were measured in fluorescence yield detection mode, recording Am Lα fluorescence radiation with a 5 pixel energy-dispersive solid-state Ge detector (Canberra LEGe). Six scans were collected and averaged. Standard data reduction and least-squares fit techniques[36] using the ATHENA[37] and UWXAFS[38] program packages were applied for EXAFS data analysis. The k^2-weighted EXAFS function $\chi(k)$ was obtained following pre-edge background subtraction, normalization, μ_0 spline function fitting, and conversion from energy to k space using the energy of the white line maximum to define the ionization energy (E_0). Metric parameters describing the Am(III) coordination (coordination numbers (N), interatomic distances (R), mean square radial displacements or EXAFS Debye−Waller factors (σ^2), and relative shifts in ionization potential (ΔE_0)) were obtained by least-squares fits of the data to the EXAFS equation. The amplitude reduction factor S_0^2 was held constant at 1.0. Theoretical scattering phase shift and backscattering amplitude functions used in the fits were obtained with the ab initio multiple-scattering code feff (v8.4)[39] based on atomic clusters derived for Eu$(NO_3)_3(C_6H_{14}O_4)$[40] and the [Ln(C5-BPP)-$(NO_3)_3$(DMF)] structure **2** (see Figure 2), where Am (Z = 95) was replaced by Eu.

Syntheses. All manipulations of air-sensitive materials were performed with rigorous exclusion of oxygen and moisture in flame-dried Schlenk-type glassware either on a dual-manifold Schlenk line, interfaced to a high-vacuum (10^{-3} Torr) line, or in an argon-filled glovebox (MBraun GmbH). Deuterated solvents (≥99 atom % D) were obtained from Eurisotop or Aldrich. Ln$(NO_3)_3\cdot 6H_2O$ was obtained from Aldrich.

Pyridine-2,6-dicarboxylic Acid Diethyl Ester. A 10.0 g amount (59.9 mmol) of pyridine-2,6-dicarboxylic acid and 2 mL of concentrated H_2SO_4 were refluxed for 3 h in 70 mL of dry ethanol and stored overnight at ambient temperature. The solvent was removed under reduced pressure. The colorless, viscous residue was dissolved in dichloromethane and neutralized with aqueous $NaHCO_3$ solution. The aqueous phase was extracted three times with 40 mL of dichloromethane. The combined organic phases were washed three times with 40 mL of water and dried with Na_2SO_4. The solvent was removed under reduced pressure, and the product was obtained as colorless crystals. Yield: 9.4 g (42.2 mmol, 70%). Melting point: 45−46.5 °C. ^{1}H NMR (400.2 MHz, methanol-d_4, 300 K): δ 1.43 (t, 6H, ^3J = 7.2 Hz, CH_3), 4.46 (q, 4H, ^3J = 7.2 Hz, CH_2), 8.14 (dd, 1H, ^3J = 8.3 Hz, ^3J = 7.3 Hz, Py H), 8.29 (d, 2H, ^3J = 7.9 Hz, Py H).

1,1′-(Pyridine-2,6-diyl)bis(5,5-dimethylhexane-1,3-dione). 4,4-Dimethylpentane-2-one (16.0 mmol, 2.3 mL) and a solution of sodium methoxide in methanol (30%, 20.0 mmol, 3.5 mL) were stirred for 30 min at room temperature under an argon atmosphere. A solution of 1.7 g (7.5 mmol) of pyridine-2,6-dicarboxylic acid diethyl ester in 40 mL of freshly distilled diethyl ether was added dropwise, and the reaction mixture was refluxed for 3 h. Subsequently it was cooled to room temperature and was neutralized with glacial acetic acid. The organic phase was washed with water (3 × 30 mL), dried with Na_2SO_4, filtered, and concentrated in vacuo. The crude product was obtained as a yellowish solid and was used without further purification. ^{1}H NMR (400.2 MHz, methanol-d_4, 300 K): δ 1.09 (s, 18H, CH_3), 2.39 (s, 4H, $CH_2C(CH_3)_3$), 6.90 (s, 4H, CH_2), 8.11 (dd, 1H, ^3J = 8.3 Hz, ^3J = 7.4 Hz, Py H), 8.23 (d, 2H, ^3J = 7.6 Hz, Py H).

2,6-Bis-(5-(2,2-dimethylpropyl)-1H-pyrazol-3-yl)-pyridine (C5-BPP). A 1.5 g amount of crude 1,1′-(pyridine-2,6-diyl)bis(5,5-dimethylhexane-1,3-dione) and 1.3 mL of hydrazine hydrate (80% in H_2O, 21 mmol) were dissolved in 150 mL of methanol and refluxed for 2 h. The solvent was removed under reduced pressure. The residue was washed with water and diethyl ether (3 × 30 mL each) and dried under reduced pressure. The product was obtained as a colorless powder. Yield (over two steps): 2.2 g, 6.4 mmol, 40%. Melting point: 259−261 °C. ^{1}H NMR (400.2 MHz, methanol-d_4, 300 K): δ 1.00 (s, 18H, H_a), 2.60 (s, 4H, H_c), 6.75 (s, 2H, H_4), 7.72 (d, 2H, ^3J = 7.7 Hz, $H_{3'}$, $H_{5'}$), 7.85 (t, 1H, ^3J = 7.7 Hz, $H_{4'}$) ppm. ^{1}H NMR (300.1 MHz, THF-d_8, 298 K): δ 0.98 (s, 18H, H_a), 2.55 (s, 4H, H_c), 6.70 (s, 2H, H_4), 7.70 (br s, 3H, $H_{3'}$, $H_{4'}$, $H_{5'}$), 11.92−12.27 (br m, 2H, NH, H_1) ppm. ^{13}C{^{1}H} NMR (75.5 MHz, THF-d_8, 298 K): δ 30.0 (C_a), 32.1 (C_b), 42.2 (C_c), 104.5 (C_4), 118.5 ($C_{3'}$, $C_{5'}$), 141.5 (C_5), 143.4 (C_3), 151.8 ($C_{2'}$, $C_{6'}$) ppm. IR (ν/cm^{-1}): 2957 (w), 1654 (w), 1574 (w), 1460 (m), 1259 (m), 1090 (m), 1012 (m), 796 (s), 753 (w), 737 (w), 661 (w). MS (EI, 70 eV, 170 °C): m/z (%) 351 [M$^+$, (11)], 336 [M$^+$ − CH_3, (6)], 294 [M$^+$ − C_4H_9, (10)], 209 [M$^+$ − $C_{10}H_{22}$, (6)], 137 [$C_8H_{13}N_2$, (26)], 71 [C_5H_{11}, (26)], 57 [C_4H_9, (45)]. HRMS: calcd for $C_{21}H_{29}N_5$, 351.2479; found, 351.1892.

[Sm(C5-BPP)$(NO_3)_3$(DMF)] (1). C5-BPP (216 mg, 0.61 mmol) and Sm$(NO_3)_3\cdot 6H_2O$ (91 mg, 0.21 mmol) were dissolved in 3 mL of DMF and stirred at 41 °C for 37 h. Then, the subsequent mixture was filtered. After removal of the solvent, the white precipitate was

dx.doi.org/10.1021/ic3000526 | Inorg. Chem. 2012, 51, 5199−5207

Scheme 3. Synthesis of C5-BPP

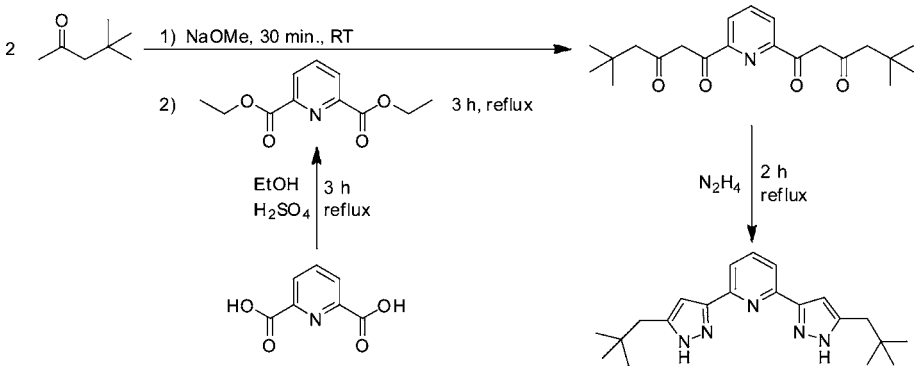

recrystallized from DMF/diethyl ether (1:10), yielding colorless crystals of **1**. Yield: 99 mg, 0.13 mmol, 64%. ^{1}H NMR (300.1 MHz, THF-d_8, 298 K): δ 0.97 (s, 18H, H_a), 2.70 (s, 4H, H_c), 2.75 (s, 3H, CH_3, DMF), 2.88 (s, 3H, CH_3, DMF), 6.66 (s, 2H, H_4), 7.95 (s, 1H, CH, DMF), 8.03 (d, ^3J = 7.7 Hz, 2H, $H_{3'}$, $H_{5'}$), 8.25 (t, ^3J = 7.7 Hz, 1H, $H_{4'}$), 10.98 (br s, 2H, H_1) ppm. ^{13}C{^{1}H} NMR (75.5 MHz, THF-d_8, 298 K): δ 29.6 (C_a), 31.1 (CH_3, DMF), 32.2 (C_b), 36.1 (CH_3, DMF), 39.6 (C_c), 103.2 (C_4), 118.5 ($C_{3'}$, $C_{5'}$), 141.4 (C_5), 144.5 (C_3), 153.4 ($C_{2'}$, $C_{6'}$), 162.6 (CHO, DMF) ppm. IR (ν/cm^{-1}): 2956 (w), 1650 (w), 1575 (w), 1462/1426 (m(sp)), 1240/1228 (m(sp)), 1115/1098 (m(sp)), 1037/1026/1010 (m(sp)), 828/812 (s(sp)), 758 (w), 736 (w), 735 (w), 675 (m). Anal. Calcd for $C_{24}H_{36}N_9O_{10}Sm$·DMF (**1**, 835.23): C, 38.88; H, 5.20; N, 16.79. Found: C, 39.19; H, 5.25; N, 16.46.

*[Eu(C5-BPP)(NO$_3$)$_3$(DMF)] (**2**).* C5-BPP (180 mg, 0.51 mmol) and $Eu(NO_3)_3$·$6H_2O$ (76 mg, 0.17 mmol) were dissolved in 3 mL of DMF and stirred at 48 °C for 120 h. Then, the subsequent mixture was filtered. After removal of the solvent, the white precipitate was recrystallized from DMF/diethyl ether (1:10) to yield colorless crystals of **2**. Yield: 116 mg, 0.15 mmol, 90%. IR (ν/cm^{-1}): 2957 (w), 1654 (w), 1574 (w), 1460 (w), 1259 (s), 1090 (s), 1012 (s), 796 (vs), 753 (w), 736 (w), 661 (w). Anal. Calcd for $C_{24}H_{36}N_9O_{10}Eu$·3DMF (**2**; 981.84): C, 40.37; H, 5.85; N, 17.12. Found: C, 40.87; H, 5.95; N, 16.88.

X-ray Crystallographic Studies of 1 and 2. Crystals of **1** and **2** were obtained from DMF/diethyl ether (1:10). A suitable crystal of compound **1** or **2** was covered in mineral oil (Aldrich) and mounted onto a glass fiber. The crystal was transferred directly to the −73 or −123 °C N_2 cold stream of a Stoe IPDS 2 diffractometer.

All structures were solved by the Patterson method (SHELXS-97).[41] The remaining non-hydrogen atoms were located from successive difference Fourier map calculations. The refinements were carried out by using full-matrix least-squares techniques on F^2, minimizing the function $(F_o - F_c)^2$, where the weight is defined as $4F_o^2/2(F_o^2)$ and F_o and F_c are the observed and calculated structure factor amplitudes using the program SHELXL-97.[41] The hydrogen atom contributions of compounds **1** and **2** were calculated but not refined. The residual electron densities in each case were of no chemical significance.

*Crystal Data for **1**:* $C_{24}H_{36}N_9O_{10}Sm$·$3C_3H_7NO$, M_r = 979.75, triclinic, a = 9.9870(6) Å, b = 16.2280(10) Å, c = 16.2640(11) Å, α = 115.420(5)°, β = 100.090(5)°, γ = 98.440(5)°, V = 2269.7(2) Å^3, T = 150(2) K, space group $P\bar{1}$, Z = 2, μ(Mo Kα) = 1.363 mm^{-1}, 42 592 reflections measured, 9644 independent reflections (R_{int} = 0.1684). The final R1 value was 0.0476 ($I > 2\sigma(I)$). The final $R_w(F^2)$ value was 0.1194 (all data). The goodness of fit on F^2 was 0.968.

*Crystal Data for **2**:* $C_{24}H_{36}N_9O_{10}Eu$·$3C_3H_7NO$, M_r = 981.87, triclinic, a = 10.074(2) Å, b = 15.930(3) Å, c = 16.520(3) Å, α = 112.71(3)°, β = 101.94(3)°, γ = 98.08(3)°, V = 2320.2(8) Å^3, T = 200(2) K, space group $P\bar{1}$, Z = 2, μ(Mo Kα) = 1.420 mm^{-1}, 18 504 reflections measured, 9545 independent reflections (R_{int} = 0.0709). The final R1 value was 0.0492 ($I > 2\sigma(I)$). The final $R_w(F^2)$ value was 0.0977 (all data). The goodness of fit on F^2 was 0.808.

Positional parameters, hydrogen atom parameters, thermal parameters, and bond distances and angles have been deposited as Supporting Information.

Liquid−Liquid Extraction. C5-BPP's performance as an extracting agent was determined by measuring the distribution of ^{241}Am(III) and ^{152}Eu(III) between an organic phase containing C5-BPP and an aqueous phase containing nitric acid, using γ counting. ^{241}Am and ^{152}Eu are radionuclides with distinctive γ lines which are easily detected. No sample preparation is required.

The organic phase was a solution of 10 mmol/L of C5-BPP + 0.5 mol/L of 2-bromohexanoic acid in kerosene prepared by dissolving weighed amounts of C5-BPP and 2-bromohexanoic acid in the diluent. The aqueous phase was ^{241}Am(III) + ^{152}Eu(III) in 0.2−2.0 mol/L HNO_3 prepared by adding 30 μL of a stock solution (60 kBq/mL ^{241}Am(III) + 100 kBq/mL ^{152}Eu(III) in 0.1 mol/L HNO_3) to 1470 μL of HNO_3.

Equal volumes (1.5 mL each) of organic and aqueous phases were contacted 45 min at 20 °C using an orbital shaker (500 rpm). It was established that 45 min was sufficient to attain equilibrium.[33] Samples were centrifuged to separate phases. ^{241}Am and ^{152}Eu activities were determined in 1.0 mL aliquots of each phase by γ counting (Packard Cobra Auto Gamma 5003).

Am(III) and Eu(III) distribution ratios $D_{Am(III)}$ and $D_{Eu(III)}$ are $D_{M(III)} = [M(III)_{org}]/[M(III)_{aq}]$. They are simply calculated from the organic phase and aqueous phase count rates of the respective radionuclide. The separation factor is $SF_{Am(III)/Eu(III)} = D_{Am(III)}/D_{Eu(III)}$. Distribution ratios (which were $10^{-3} < D < 10^3$, see Results and Discussion) typically are reproducible within ±20%.[42]

TRLFS Titration. The TRLFS titration experiments were performed using a stock solution of 6.67 × 10^{-6} mol/L Cm(III) (89.7% ^{248}Cm, 0.1% ^{247}Cm, 9.4% ^{246}Cm, 0.1% ^{245}Cm, 0.3% ^{244}Cm, and 0.4% ^{243}Cm) in 0.03 mol/L of $HClO_4$. A 15 μL portion of the Cm stock solution was dissolved in 985 μL of methanol. The initial Cm(III) concentration was 1.0 × 10^{-7} mol/L. Ligand solutions were prepared by dissolving 3.51 mg of C5-BPP in 985 μL of methanol and subsequent dilution with 15 μL of distilled water (to maintain a constant water content during titration), resulting in a 10^{-2} mol/L stock solution. For the titration experiments C5-BPP solutions with concentrations between 10^{-6} and 10^{-2} mol/L were prepared and successively added. The resulting solutions were allowed to equilibrate for 10 min before measurement to ensure equilibration. The C5-BPP concentration ranged from 0 to 4.68 × 10^{-3} mol/L.

EXAFS Sample Preparation. The Am(III)-C5-BPP complex was measured in solution. A 35 μL portion of an Am(III) stock solution (aqueous 0.5 M HNO_3 solution containing 30 MBq/mL of ^{243}Am and 17 MBq/mL of ^{241}Am, corresponding to 17 mmol/L of Am) was gently heated in a glass vial to near dryness and then 300 μL of 10 mmol/L C5-BPP in 2-propanol added (2-propanol had to be used instead of methanol because of limited solubility; however, the complexation properties of methanol and 2-propanol are quite similar). A 250 μL amount of the resulting solution (2 mmol/L of Am), sample **3**, was transferred to a polypropylene-capped vial, the cap

dx.doi.org/10.1021/ic3000526 | Inorg. Chem. 2012, 51, 5199−5207

sealed shut with epoxy glue, and the sealed vial placed in the INE-Beamline standard sample containment chamber for measurement.

RESULTS AND DISCUSSION

Ligand Synthesis. C5-BPP was synthesized in three steps (Scheme 3) starting from pyridine-2,6-dicarboxylic acid, which was converted to the corresponding diethyl ester in the first step. In a Claisen condensation the diethyl ester was treated with 4,4-dimethylpentan-2-one in the presence of sodium methoxide to give the corresponding β-diketone, which was reacted without further purification with hydrazinium hydrate in CH_2Cl_2 to give the desired product C5-BPP in good yield. The purity of the desired product was confirmed by ^1H and $^{13}C\{^1H\}$ NMR spectroscopy.

Liquid–Liquid Extraction. Prior screening tests have shown that, in contrast to BTP[7,8] and BTBP,[11] C5-BPP does not extract Am(III) and Eu(III) nitrates from nitric acid by solvation according to

$$M^{3+}_{aq} + 3NO_3^-{}_{aq} + n\text{C5-BPP}_{org} \rightarrow M(NO_3)_3(\text{C5-BPP})_{n\ org}$$

However, C5-BPP does extract Am(III) with high selectivity over Eu(III) in the presence of a lipophilic anion source such as a 2-bromocarboxylic acid by a cation-exchange mechanism:[32,33]

$$M^{3+}_{aq} + n\text{C5-BPP}_{org} + 3HA_{org} \rightleftharpoons MA_3(\text{C5-BPP})_{n\ org} + 3H^+_{aq}$$

The dependence of Am(III) and Eu(III) distribution ratios and the separation factor on nitric acid concentration is shown in Figure 1. Am(III) is extracted (i.e., $D_{Am(III)} > 1$) from <1 mol/L nitric acid under the experimental conditions used. The selectivity for Am(III) over Eu(III) is very good, in the range of $SF_{Am(III)/Eu(III)} \approx 100$, which lies in the range of separation factors found for BTP and BTBP.[7,8,11] Am(III) back-extraction (i.e., $D_{Am(III)} < 1$) requires a nitric acid concentration of >1 mol/L. Unfortunately, a precipitate occurs for ≥1.3 mol/L nitric acid. Nevertheless, a more complete solvent extraction study[33] shows that the precipitation issue is solved by modifying the diluent. The C5-BPP ligand also shows good chemical stability toward high nitric acid concentrations and fast extraction kinetics. This study also reveals that slope analysis is not suitable to determine the composition of the extracted complexes, due to strong ligand aggregation and ligand–ligand interaction.

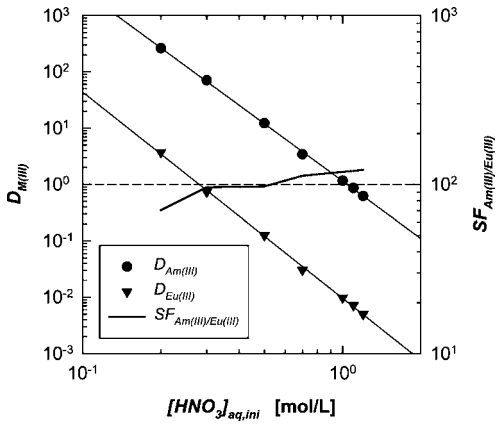

Figure 1. Extraction of Am(III) and Eu(III): dependence of Am(III) and Eu(III) distribution ratios and separation factor on initial nitric acid concentration. Aqueous phase: ^{241}Am(III) + ^{152}Eu(III) in HNO_3. T = 293 K.

The slopes for log $D_{Am(III)}$ and log $D_{Eu(III)}$ vs log $[HNO_3]$ are −3.4 and −3.6, respectively. This is in agreement with a cation-exchange mechanism, where a slope of 3 is expected for log $D_{Am(III)}$ or log $D_{Eu(III)}$ vs pH. The steeper slopes in Figure 1 are likely due to the fact that distribution ratios are simply plotted vs the nitric acid concentration without taking into account activity coefficients.

To our knowledge, these results show that C5-BPP is able to extract Am(III) from more acidic solutions with better selectivity over Eu(III) than any other N-donor extracting agent in combination with 2-bromocarboxylic acid.[4]

Sm(III) and Eu(III) Complex Structures. Stirring a 3:1 mixture of C5-BPP with $Ln(NO_3)_3{\cdot}6H_2O$ (Ln = Sm(III), Eu(III)) in DMF at elevated temperature for a prolonged time did not result in the formation of complexes with the central metal ion coordinated by three ligands. Instead, the monoligated compounds $[Ln(\text{C5-BPP})(NO_3)_3(DMF)]$ (Ln = Sm(III) (**1**), Eu(III) (**2**)) were obtained as colorless crystals after recrystallization from DMF/diethyl ether (1:10) (Scheme 4). These results are in contrast with those for the related ligand 2,6-bis(1*H*-pyrazol-3-yl)pyridine with $LnCl_3{\cdot}6H_2O$ (Ln = Eu(III), Gd(III), Tb(III), Ho(III)) in methanol, which upon treatment with KPF_6 yields complexes with three ligands coordinating to the lanthanide atom.[43] Obviously, the 2,6-bis(1*H*-pyrazol-3-yl)pyridine ligand substitutes water molecules of the lanthanides atoms but not the NO_3^- anions (see below for the solid-state data). Similar observations were recently made using 6-(3,5-dimethyl-1*H*-pyrazol-1-yl)-2,2′-bipyridine (dmpbipy) as ligand;[34] in this case NO_3^- anions were also not replaced. This observation is significant, since the separation of actinides from lanthanides, e.g., in the SANEX process, is usually performed in HNO_3 solutions.

The new complexes were characterized by standard analytical and spectroscopic techniques, and the solid-state structure was established by single-crystal X-ray diffraction. As result of the paramagnetic metals only NMR data of compound **1** could be obtained. As expected, the peaks are broadened. Most characteristic are the signals of the *t*Bu group of the alkyl

Scheme 4. Synthesis of 1 and 2

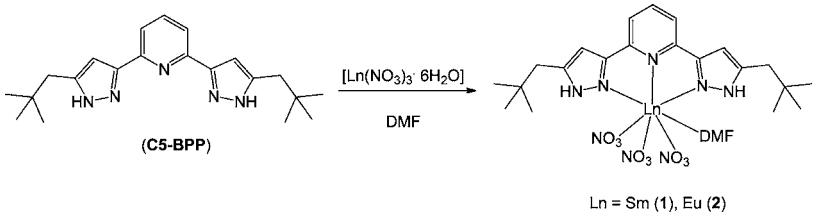

dx.doi.org/10.1021/ic3000526 | Inorg. Chem. 2012, 51, 5199–5207

chain, which are observed at $\delta(^1H)$ 0.78 ppm and $\delta(^{13}C\{^1H\})$ 32.5 ppm, only slightly shifted from the values observed for noncoordinated C5-BPP. In the aromatic region two typical signals for the pyridine ring and one signal for the pyrazolyl ring were observed.

Compounds **1** and **2** are isostructural, both crystallizing in the triclinic space group $P\bar{1}$ and having two molecules of the complex in the unit cell (Figure 2). The central metals are 10-fold coordinated by three κ^2O,O'-NO_3^- groups, the tridentate C5-BPP ligand, and one DMF molecule, forming a distorted hexadecahedron (see Figure S1 in the Supporting Information).[44] The Ln−O bond distances of the nitro groups are within the expected ranges of 2.518(3)−2.604(4) Å (**1**) and 2.478(4)−2.549(5) (**2**) Å.[34] The bite angles of the C5-BPP ligand are N2−Ln−N3 = 62.65(11)° (**1**) and 62.38(14)° (**2**), N2−Ln−N4 = 124.81(11)° (**1**) and 124.70(14)° (**2**), and N3−Ln−N4 = 62.45(11)° (**1**) and 62.41(14)° (**2**). The Ln−N bond length of the pyridine ring (Ln−N3 = 2.628(3) Å (**1**), 2.622(4) Å (**2**)) is slightly longer than the Ln−N bond distances of the five-membered pyrazolyl ring (Ln−N2 = 2.548(4) Å (**1**) and 2.545(4) Å (**2**), Ln−N4 = 2.584(4) Å (**1**) and 2.541(5) Å (**2**)). A comparison of compound **2** with the 9-fold coordinated tris(2,6-bis(1*H*-pyrazol-3-yl)pyridine)europium cation[43] does not reveal any significant differences in their Eu−N bond distances.

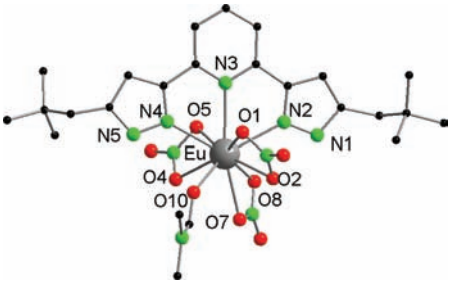

Figure 2. Solid-state structure of **2** showing the atom-labeling scheme, omitting hydrogen atoms. Selected bond lengths (Å) and angles (deg) (also given for the isostructural compound **1**): Eu−O1 = 2.478(4), Eu−O2 = 2.551(4), Eu−O4 = 2.503(4), Eu−O5 = 2.520(4), Eu−O7 = 2.549(5), Eu−O8 = 2.550(4), Eu−O10 = 2.388(4), Eu−N2 = 2.545(4), Eu−N3 = 2.622(4), Eu−N4 = 2.541(5); N2−Eu−N3 = 62.38(14), N2−Eu−N4 = 124.70(14), N3−Eu−N4 = 62.41(14); Sm−O1 = 2.518(3), Sm−O2 = 2.525(4), Sm−O4 = 2.594(3), Sm−O5 = 2.545(4), Sm−O7 = 2.604(4), Sm−O8 = 2.497(3), Sm−O10 = 2.348(3), Sm−N2 = 2.548(4), Sm−N3 = 2.628(3), Sm−N4 = 2.583(4); N2−Sm−N3 = 62.65(11), N2−Sm−N4 = 124.81(11), N3−Sm−N4 = 62.45(11).

TRLFS. The evolution of the Cm(III) fluorescence emission resulting from the $^6D'_{7/2} \rightarrow {}^8S'_{7/2}$ transition in methanol (containing 3.3 mol % of water from the Cm(III) stock solution) and in the presence of increasing amounts of C5-BPP is shown in Figure 3. The spectra are normalized to the same peak area for better comparison. At zero ligand concentration a broad emission band at 599.3 nm with a shoulder at 603.7 nm is observed, which originate from different $[Cm(solv)]^{3+}$ species with varying numbers of methanol and/or water molecules in the inner coordination sphere. According to ref 45, the spectrum of $[Cm(solv)]^{3+}$ results from two different species with nine methanol and eight methanol/one water molecules in the inner coordination sphere, respectively. With increasing C5-BPP concentration the emission band shifts to higher wavelength, displaying distinct emission maxima at

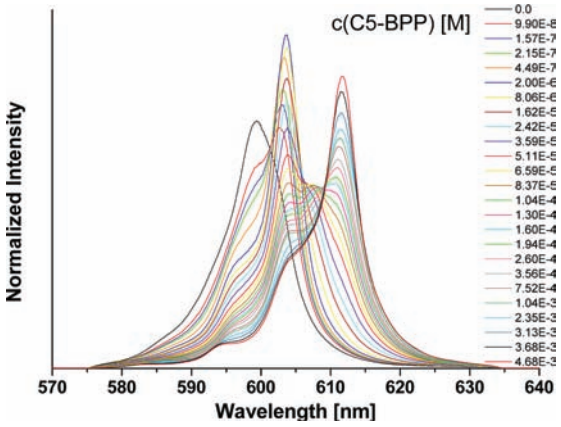

Figure 3. Normalized fluorescence spectra of Cm(III) in methanol with increasing C5-BPP concentration. $[Cm(III)]_{ini} = 1 \times 10^{-7}$ mol/L; [C5-BPP] = (0−4.68) × 10^{-3} mol/L.

603.7, 607.7, and 611.6 nm. The emission band of the $[Cm(solv)]^{3+}$ species decreases simultaneously. The spectroscopic results show that three different Cm-C5-BPP species are formed in the ligand concentration range of 9.9 × 10^{-8}−4.7 × 10^{-3} mol/L. These are attributed to the 1:1, 1:2, and 1:3 $[Cm(C5\text{-}BPP)_n]^{3+}$ complexes with n = 1−3 (see below).

The fluorescence spectra are analyzed by peak deconvolution using the spectra of the four single components ($[Cm(solv)]^{3+}$ and $[Cm(C5\text{-}BPP)_n]^{3+}$; n = 1−3) displayed in Figure 4. The resulting speciation diagram is shown in Figure 5.

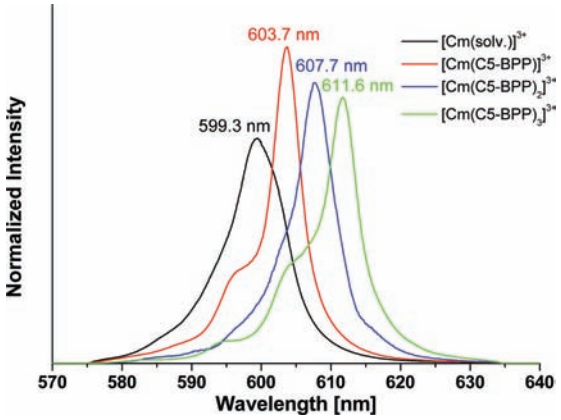

Figure 4. Normalized fluorescence spectra of the pure components $[Cm(solv)]^{3+}$ and $[Cm(C5\text{-}BPP)_n]^{3+}$ (n = 1−3).

At low ligand concentrations $[Cm(solv)]^{3+}$ is the dominant species. With increasing C5-BPP concentration the 1:1 Cm-C5-BPP complex is formed and dominates in the concentration range 2 × 10^{-7}−3 × 10^{-5} mol/L. At concentrations greater than 10^{-4} mol/L the 1:3 Cm-C5-BPP complex is the dominant species. In the concentration range 10^{-6}−10^{-3} mol/L the 1:2 Cm-C5-BPP complex is also present, with a relative fraction of approximately 40% at 10^{-4} mol/L. Figure 5 also includes the relative species distribution calculated with the log K_n (n = 1−3) values determined below. Comparison with the experimental data shows an excellent agreement in the concentration range 10^{-7}−2 × 10^{-4} mol/L. At the highest ligand concentrations studied, the experimental values differ significantly from the calculated curve, which is due to colloid formation observed for [C5-BPP] ≥ 10^{-4} mol/L.

dx.doi.org/10.1021/ic3000526 | *Inorg. Chem.* 2012, 51, 5199−5207

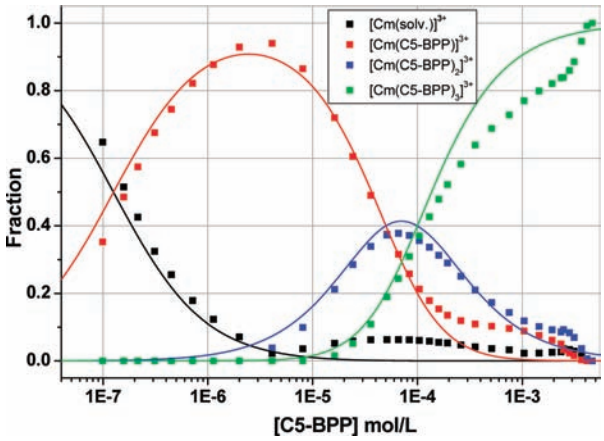

Figure 5. Relative Cm(III) species concentrations in methanol as a function of the total C5-BPP concentration. Symbols give experimental data from peak deconvolution. Lines designate relative species calculated with log K_1 = 6.9, log K_2 = 4.3, and log K_3 = 3.6.

Stepwise formation of the 1:1, 1:2, and 1:3 Cm-C5-BPP complexes is described by eq 1. To ascertain the stoichiometry

$$[\mathrm{Cm(solv)}]^{3+} \underset{-\mathrm{C5\text{-}BPP}}{\overset{+\mathrm{C5\text{-}BPP}}{\rightleftharpoons}} [\mathrm{Cm(C5\text{-}BPP)}]^{3+} \underset{-\mathrm{C5\text{-}BPP}}{\overset{+\mathrm{C5\text{-}BPP}}{\rightleftharpoons}} [\mathrm{Cm(C5\text{-}BPP)_2}]^{3+} \underset{-\mathrm{C5\text{-}BPP}}{\overset{+\mathrm{C5\text{-}BPP}}{\rightleftharpoons}} [\mathrm{Cm(C5\text{-}BPP)_3}]^{3+} \quad (1)$$

of the $[\mathrm{Cm(C5\text{-}BPP)}_n]^{3+}$ (n = 1−3) complexes, the logarithm of the concentration ratio $[\mathrm{Cm(C5\text{-}BPP)}_n]^{3+}/[\mathrm{Cm(C5\text{-}BPP)}_{n-1}]^{3+}$ (n = 1−3) is plotted as a function of log [C5-BPP] according to eq 2.

$$\log\left(\frac{[\mathrm{Cm(C5\text{-}BPP)}_n]^{3+}}{[\mathrm{Cm(C5\text{-}BPP)}_{n-1}]^{3+}}\right) = \log K + n \log[\mathrm{C5\text{-}BPP}] \quad (n = 1-3) \quad (2)$$

The double-logarithmic plot of the concentration ratios is shown in Figure 6. The free ligand concentration is determined from the initial ligand concentration in due consideration of the fraction of the complexed species. Slopes of 0.96 ± 0.05, 0.93 ± 0.04, and 0.94 ± 0.05 are derived by linear regression for the stepwise formation of the $[\mathrm{Cm(C5\text{-}BPP)}_n]^{3+}$ complexes (n = 1−3). These results are in excellent agreement with the model described by eq 1 and confirm the unambiguous assignment of the three observed species with emission maxima at 603.7, 607.7, and 611.6 nm to be the 1:1, 1:2, and 1:3 Cm-C5-BPP complexes, respectively.

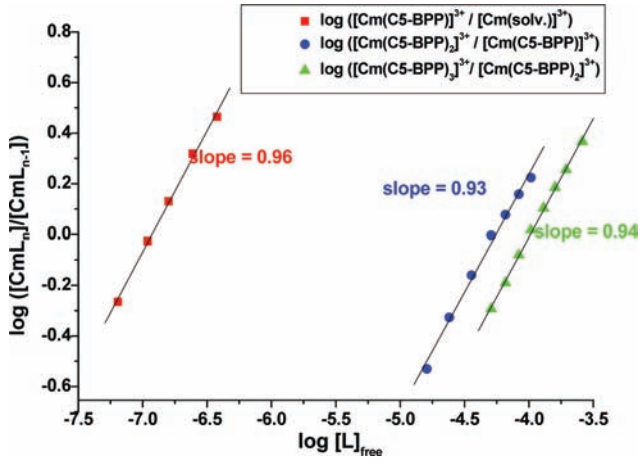

Figure 6. Double-logarithmic plots of $[\mathrm{Cm(C5\text{-}BPP)}_n]^{3+}/[\mathrm{Cm(C5\text{-}BPP)}_{n-1}]^{3+}$ (n = 1−3) concentration ratios versus free C5-BPP concentration.

The conditional stability constants log K_n (n = 1−3) for the stepwise complexation of Cm(III) with C5-BPP are calculated according to eq 3.

$$K_n = \frac{[\mathrm{Cm(C5\text{-}BPP)}_n]^{3+}}{[\mathrm{Cm(C5\text{-}BPP)}_{n-1}]^{3+}[\mathrm{C5\text{-}BPP}]} \quad (3)$$

Average values of log K_1 = 6.9 ± 0.2, log K_2 = 4.3 ± 0.1, and log K_3 = 3.6 ± 0.1 are determined from the spectroscopic data, resulting in stability constants of log β_2 = 11.2 ± 0.3 and log β_3 = 14.8 ± 0.4 for the 1:2 and the 1:3 Cm(III)-C5-BPP complexes. In a previous study[34] using a similar ligand, dmpbipy, only the 1:1 Cm(III)-dmpbipy complex formed in 1-octanol solution, having the conditional stability constant log K_1 = 2.80 ± 0.02. This difference mirrors dmpbipy's inferior behavior as an extracting agent.

A stability constant of log β_3 = 14.4 ± 0.1 was found for the Cm(III)-BTP 1:3 complex.[26] This value is similar to that reported here for C5-BPP but was determined using a different diluent to dissolve the ligand (water/methanol 1:1 instead of methanol for C5-BPP). The weaker coordination of methanol compared to that of water is expected to cause an increase in the value of the stability constant for C5-BPP. Nevertheless, the Cm(III) TRLFS results indicate that BTP and C5-BPP show similar affinity for Cm(III).

Similar results have been observed for Eu(III)-C5-BPP complexes in solution. The Eu(III) fluorescence spectra resulting from the $^5D_0 \rightarrow {}^7F_1$ and $^5D_0 \rightarrow {}^7F_2$ transitions in the presence of increasing amounts of C5-BPP are displayed in Figure S5 (Supporting Information). The spectroscopic results show that four different Eu(III) species are formed in the ligand concentration range of (0−3.5) × 10^{-3} mol/L. In accordance with the Cm(III) results, these species are attributed to the $[\mathrm{Eu(solv)}]^{3+}$ and the 1:1, 1:2, and 1:3 $[\mathrm{Eu(C5\text{-}BPP)}_n]^{3+}$ complexes with n = 1−3. Due to the small shifts in the Eu(III) fluorescence spectra, a quantitative determination of the four individual species was not possible. Nevertheless, the 1:3 $[\mathrm{Eu(C5\text{-}BPP)_3}]^{3+}$ complex which forms at a ligand concentration of >1 × 10^{-3} mol/L was verified by fluorescence lifetime measurements. In the course of the titration the fluorescence lifetime increases from 182 μs ($[\mathrm{Eu(solv)}]^{3+}$ complex) to 2262 μs. According to ref 46, the fluorescence lifetime corresponds to a 9-fold coordination of Eu(III), confirming the formation of the $[\mathrm{Eu(C5\text{-}BPP)_3}]^{3+}$ complex. In comparison to the case for Cm(III), considerably higher ligand concentrations are required for a quantitative formation of the 1:3 complex. This is in good agreement with the results of the extraction experiments displaying the separation factors $SF_{\mathrm{Am(III)/Eu(III)}} \approx 100$.

EXAFS Analysis. The Am L3-EXAFS of sample **3** ([Am] = 2 mmol/L, [C5-BPP] = 10 mmol/L in 2-propanol) is depicted in Figure 7. The transformation range and metric parameters obtained from fits are summarized in Table 1.

dx.doi.org/10.1021/ic3000526 | Inorg. Chem. 2012, 51, 5199−5207

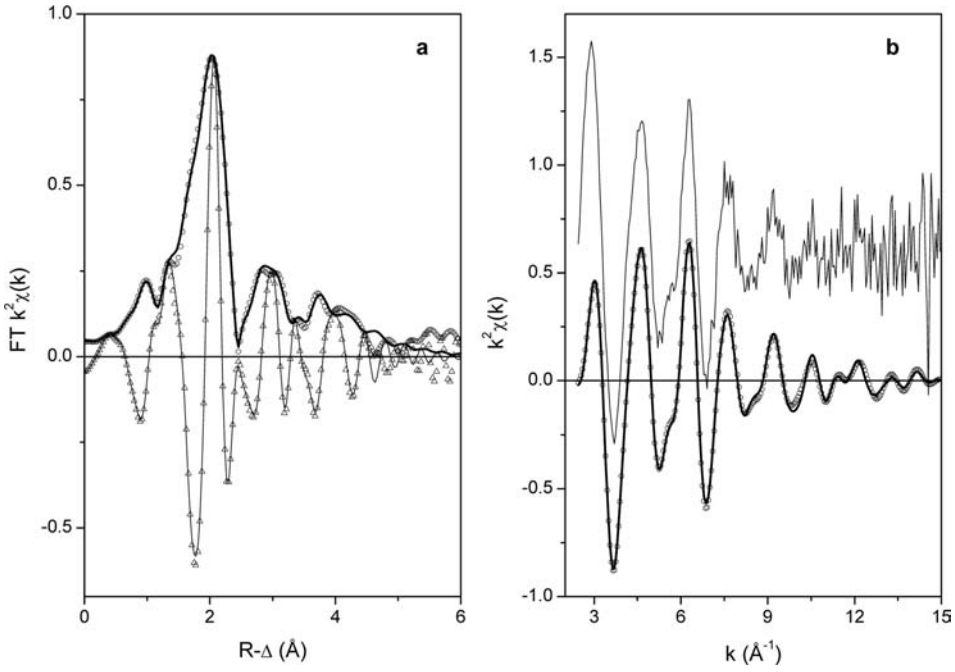

Figure 7. Am L3-EXAFS for Am(III)-C5-BPP, sample **3**: (a) experimental Fourier transform (FT) magnitude (circles) and real part (triangles), with solid lines giving theoretical curves from fit results; (b) experimental k^2-weighted data (thin solid line, vertically shifted for clarity), back-transformed data (circles), and theoretical fit curve (solid line).

Table 1. EXAFS Fit Parameters: ΔE_0 Global Parameter (g) for All Shells, with S02 Fixed at 1.0[a]

k range (Å^{-1}) fit range (Å)	shell	N	R (Å)	ΔE_0 (eV)	σ^2 (Å^2)	r factor (%)
2.45−14.95	O(N)	9.5	2.54(1)	−6.88 (g)	0.0084	0.4
1.45−4.75	N(C)	8.5	2.78(2)		0.0107	
	C(N)	12.9	3.77(3)		0.0069	
	O_{dist}	9.3	4.16(3)		0.0053	

[a]Errors in coordination numbers are estimated to be 10% for the first two shells and 20−40% for higher shells.

Three peaks are discernible from the FT magnitude—at ∼2, 2.9, and 4 Å (non-phase-shift-corrected $R - \Delta$ values). These peaks are due to scattering paths between the central Am(III) cation and ligand atoms, potentially coordinating oxygen atoms from nitrate groups, or coordinating nitrogen atoms from pyrazolyl and pyridine rings for the first shell, nitrogen atoms from coordinating nitrate groups for the second shell, and either further distant C and N atoms from coordinating C5-BPP ligands or distal nitrate oxygen atoms comprising the third shell. Two factors complicate EXAFS fit analysis of the experimental $\chi(k)$ function: N, O, and C are indistinguishable as backscattering atoms, while the effect of multiple scattering (mainly triangular) paths in a highly symmetric metal−organic complex coordination environment, as observed for, e.g., Am(III)-BTP_3,[21] cannot be ruled out.

Several models were tested to reproduce the experimental EXAFS $\chi(k)$ function:

(1) a simulation assuming a symmetric Am(III)$(C5\text{-}BPP)_3$ coordination
(2) a cluster containing only coordinated nitrate groups in a structure derived from ref 40
(3) a 32-atom cluster derived from structure **2** containing Am(III) as central atom
(4) a peak by peak fit based on single and double scattering paths calculated for the first and the second model

The following conclusions can be drawn from attempts to fit the data using these models: neither models 1 and 3 nor the exclusive nitrate coordination according to model 2 satisfactorily reproduces the experimental data over the full k range. Only the first FT peak at ∼2 Å ($R - \Delta$) is well reproduced using model 3. A single-path fit of the first shell FT peak yields 9−10 N/O at an average distance of 2.54 Å, in agreement with the structures of compounds **1** and **2**. The rather large Debye−Waller factor of 0.0085 Å^2 reflects structural disorder due to varying bond distances between Am(III) and coordinating oxygen atoms from nitrate groups and coordinating N atoms from pyrazolyl and pyridine rings. Simulations using the feff code indicated that the second FT peak (∼2.9 Å ($R - \Delta$)) includes intensity from the central N atoms of coordinating nitrate groups (up to seven, assuming coordination by a single C5-BPP ligand) and, to a minor extent, from carbon atoms adjacent to coordinating N atoms in the rings. A single path fit yields a total of eight to nine N/C backscatterers at an average distance of 2.78 Å. Again the large σ^2 value is indicative of asymmetric coordination in this shell by the two different types of ligands. The third FT peak comprises contributions from further distant C and (noncoordinated) N atoms of C5-BPP but seems to be dominated by backscattering from the distal oxygen atoms of coordinating nitrate groups. This signal is likely enhanced by the focusing effect (three-legged paths) of the central nitrate N atom in the nearly linear Am(III)−N−O_{dist} arrangement. Aside from this, multiple scattering paths

dx.doi.org/10.1021/ic3000526 | Inorg. Chem. 2012, 51, 5199−5207

seem to play a minor role and were not considered. Any coordination of solvent 2-propanol molecules cannot be ruled out, as they are not unambiguously discernible from the EXAFS data.

In summary, the EXAFS analysis of the Am(III)-C5-BPP complex (sample **3**) indicates a $[Am(C5\text{-}BPP)(NO_3)_3]$ structure similar to structures **1** and **2**. Considering the similar behaviors of Am(III) and Cm(III) and the total C5-BPP concentration of 10 mmol/L, one would however expect the formation of the 1:3 complex according to the TRLFS results (cf. Figure 5). This discrepancy is explained by the presence of HNO_3 in the Am(III) sample (**3**), which competes with Am(III) for the C5-BPP ligand. A TRLFS experiment was performed, adding increasing concentrations of HNO_3 to a sample initially containing exclusively the 1:3 complex (at 611.4 nm). The result clearly demonstrates a transition to the 1:1 complex (at 603.2 nm; Figure 8). The peak at 615.0 nm, not

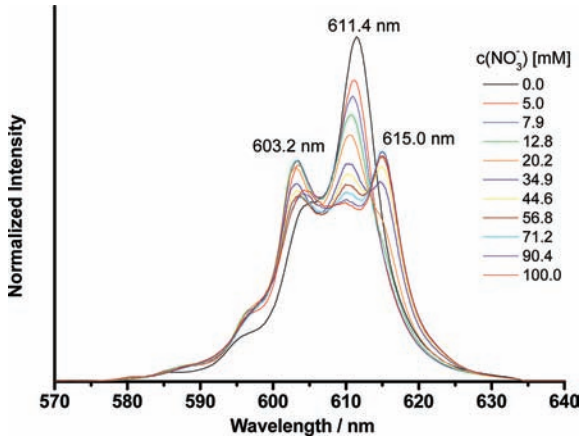

Figure 8. Normalized fluorescence spectra of Cm(III) in methanol with increasing HNO_3 concentration. $[Cm(III)]_{ini} = 1 \times 10^{-7}$ mol/L; $[C5\text{-}BPP]_{ini} = 5 \times 10^{-3}$ mol/L; $[HNO_3] = 0-0.1$ mol/L.

observed in the spectra shown in Figure 5, may be due to the formation of a 1:3 complex with a coordinating nitrate anion. A similar mixed ligand/nitrate species was found for BTP under specific conditions; this species too has a Cm(III) fluorescence emission peak which is red-shifted approximately 4 nm from that of the symmetric 1:3 complex.

CONCLUSION

C5-BPP initially was synthesized and tested as a selective extracting agent for trivalent actinides. Due to its good performance as a selective extracting agent with structural similarity to BTP, C5-BPP's complexing properties were studied from a fundamental point of view.

The solid-state structures of the isostructural lanthanide complexes $[Ln(C5\text{-}BPP)(NO_3)_3(DMF)]$ (Ln = Sm(III) (**1**), Eu(III) (**2**)) were determined and compared to the solution structure of the Am(III) 1:1 complex $[Am(C5\text{-}BPP)(NO_3)_3]$ (**3**); similar average bond lengths in the first coordination sphere of 2.54 Å were found. This is in agreement with results regarding the bond lengths in actinide(III)- and lanthanide-(III)-BTP complexes.[18,21,25]

The stability constant of the 1:3 Cm(III)-C5-BPP complex ($\log \beta_3 = 14.8 \pm 0.4$) is similar to that of the 1:3 Cm(III)-BTP complex ($\log \beta_3 = 14.4 \pm 0.1$).[26] While BTP extracts trivalent actinide nitrates, weaker ligands such as dmpbipy[34] require a carboxylic acid as a lipohilic anion source. Despite its high complexation strength, C5-BPP also requires a lipohilic anion source. This implies that differences regarding the extractability of actinide(III) and lanthanide(III) nitrates do not originate from differences in ligand strength. Further fundamental studies on the extractability of trivalent actinide nitrates are strongly required.

We plan to continue varying the structure of N-donor ligands systematically to identify trends in complex stability and extractability. Also, understanding the difference between BTP/BTBP and BPP (the former extract actinide nitrates, whereas the latter extract only the more lipophilic actinide 2-bromocarboxylates) is part of these studies. Future research and development on new N-donor extracting agents for separating actinides(III) from lanthanides(III) in the context of nuclear fuel cycles should focus on finding complexes which can accommodate nitrate anions required for charge compensation in a rather hydrophobic environment. In this context, the results are of major importance for an understanding of the extraction mechanism on a molecular level and are essential for the intelligent design of improved extractants for future industrial processing of used nuclear fuels.

ASSOCIATED CONTENT

Supporting Information

X-ray crystallographic files in CIF format for the structure determinations of **1** and **2**, ORTEP plots, and a figure showing the coordination polyhedron. This material is available free of charge via the Internet at http://pubs.acs.org.

AUTHOR INFORMATION

Corresponding Author

*E-mail: andreas.geist@kit.edu (A.G.).

Present Address

⊥Novartis Institute for BioMedical Research, CH-4002 Basel, Switzerland.

Notes

The authors declare no competing financial interest.

ACKNOWLEDGMENTS

This work was supported by the German Federal Ministry of Education and Research (BMBF) under contract numbers 02NUK012A, 02NUK012B, and 02NUK012D, the Baden-Württemberg Stiftung gGmbH, Energie Baden-Württemberg (EnBW-Stiftung), and the Commission of the European Community (project ACTINET-I3). We thank Dr. Ralf Köppe for performing the DFT studies of the ligand.

REFERENCES

(1) OECD/NEA, Status and Assesment Report on Actinide and Fission Product Partitioning and Transmutation. Paris, 1999.

(2) Magill, J.; Berthou, V.; Haas, D.; Galy, J.; Schenkel, R.; Wiese, H.-W.; Heusener, G.; Tommasi, J.; Youinou, G. *Nuclear Energy* **2003**, *42*, 263–277.

(3) Salvatores, M.; Palmiotti, G. *Prog. Part. Nucl. Phys.* **2011**, *66*, 144–166.

(4) Kolarik, Z. *Chem. Rev.* **2008**, *108*, 4208–4252 and references therein.

(5) Ekberg, C.; Fermvik, A.; Retegan, T.; Skarnemark, G.; Foreman, M. R. S.; Hudson, M. J.; Englund, S.; Nilsson, M. *Radiochim. Acta* **2008**, *96*, 225–233.

(6) Kolarik, Z.; Müllich, U.; Gassner, F. *Solvent Extr. Ion Exch.* **1999**, *17*, 23–32.

(7) Kolarik, Z.; Müllich, U.; Gassner, F. *Solvent Extr. Ion Exch.* **1999**, *17*, 1155−1170.
(8) Trumm, S.; Geist, A.; Panak, P. J.; Fanghänel, Th. *Solvent Extr. Ion Exch.* **2011**, *29*, 213−229.
(9) Drew, M. G. B.; Foreman, M. R. S.; Hudson, M. J.; Madic, C. *Inorg. Chem. Commun.* **2005**, *8*, 239−241.
(10) Foreman, M. R. S.; Hudson, M. J.; Geist, A.; Madic, C.; Weigl, M. *Solvent Extr. Ion Exch.* **2005**, *23*, 645−662.
(11) Geist, A.; Hill, C.; Modolo, G.; Foreman, M. R. S.; Weigl, M.; Gompper, K.; Hudson, M. J.; Madic, C. *Solvent Extr. Ion Exch.* **2006**, *24*, 463−483.
(12) Lewis, F. W.; Harwood, L. M.; Hudson, M. J.; Drew, M. G. B.; Desreux, J. F.; Vidick, G.; Bouslimani, N.; Modolo, G.; Wilden, A.; Sypula, M. *J. Am. Chem. Soc.* **2011**, *133*, 13093−13102.
(13) Drew, M. G. B.; Guillaneux, D.; Hudson, M. J.; Iveson, P. B.; Russell, M. L.; Madic, C. *Inorg. Chem. Commun.* **2001**, *4*, 12−15.
(14) Iveson, P. B.; Rivière, C.; Guillaneux, D.; Nierlich, M.; Thuéry, P.; Ephritikhine, M.; Madic, C. *Chem. Commun.* **2001**, 1512−1513.
(15) Berthet, J. C.; Miquel, Y.; Iveson, P. B.; Nierlich, M.; Thuéry, P.; Madic, C.; Ephritikhine, M. *Dalton Trans.* **2002**, 3265−3272.
(16) Guillaumont, D. *J. Phys. Chem. A* **2004**, *108*, 6893−6900.
(17) Colette, S.; Amekraz, B.; Madic, C.; Berthon, L.; Cote, G.; Moulin, C. *Inorg. Chem.* **2004**, *43*, 6745−6751.
(18) Denecke, M. A.; Rossberg, A.; Panak, P. J.; Weigl, M.; Schimmelpfennig, B.; Geist, A. *Inorg. Chem.* **2005**, *44*, 8418−8425.
(19) Foreman, M. R. S.; Hudson, M. J.; Drew, M. G. B.; Hill, C.; Madic, C. *Dalton Trans.* **2006**, 1645−1653.
(20) Hudson, M. J.; Boucher, C. E.; Braekers, D.; Desreux, J. F.; Drew, M. G. B.; Foreman, M. R. S.; Harwood, L. M.; Hill, C.; Madic, C.; Marken, F.; Youngs, T. G. A. *New J. Chem.* **2006**, *30*, 1171−1183.
(21) Denecke, M. A.; Panak, P. J.; Burdet, F.; Weigl, M.; Geist, A.; Klenze, R.; Mazzanti, M.; Gompper, K. *C. R. Chimie* **2007**, *10*, 872−882.
(22) Steppert, M.; Walther, C.; Geist, A.; Fanghänel, Th. *New J. Chem.* **2009**, *33*, 2437−2442.
(23) Retegan, T.; Berthon, L.; Ekberg, C.; Fermvik, A.; Skarnemark, G.; Zorz, N. *Solvent Extr. Ion Exch.* **2009**, *27*, 663−682.
(24) Trumm, S.; Lieser, G.; Foreman, M. R. S.; Panak, P. J.; Geist, A.; Fanghänel, Th. *Dalton Trans.* **2010**, *39*, 923−929.
(25) Banik, N. L.; Schimmelpfennig, B.; Marquardt, C. M.; Brendebach, B.; Geist, A.; Denecke, M. A. *Dalton Trans.* **2010**, *39*, 5117−5122.
(26) Trumm, S.; Panak, P. J.; Geist, A.; Fanghänel. *Eur. J. Inorg. Chem.* **2010**, 3022−3028.
(27) Hubscher-Bruder, V.; Haddaoui, J.; Bouhroum, S.; Arnaud-Neu, F. *Inorg. Chem.* **2010**, *49*, 1363−1371.
(28) Rawat, N.; Bhattacharyya, A.; Ghosh, S. K.; Gadly, T.; Tomar, B. S. *Radiochim. Acta* **2011**, *99*, 705−712.
(29) Steppert, M.; Císařová, I.; Fanghänel, Th.; Geist, A.; Lindqvist-Reis, P.; Panak, P. J.; Štěpnička, P.; Trumm, S.; Walther, C. *Inorg. Chem.* **2012**, *51*, 591−600.
(30) Gal, M.; Tarrago, G.; Steel, P.; Marzin, C. *Nouv. J. Chim.* **1985**, *9*, 617−620.
(31) Halcrow, M. A. *Coord. Chem. Rev.* **2005**, *249*, 2880−2908.
(32) Geist, A.; Müllich, U.; Karpov, A.; Zevaco, T.; Müller, T. DE 10 2009 003 783, 2009.
(33) Geist, A.; Müllich, U.; Wilden, A.; Gülland, S.; Modolo, G. Proc. 19th International Solvent Extraction Conference (ISEC 2011), 3−7 October 2011, Santiago de Chile.
(34) Girnt, D.; Roesky, P. W.; Geist, A.; Ruff, C.; Panak, P. J.; Denecke, M. A. *Inorg. Chem.* **2010**, *49*, 9627−9635.
(35) Denecke, M. A.; Rothe, J.; Dardenne, K.; Blank, H.; Hormes. *J. Phys. Scr.* **2005**, *T115*, 1001−1003.
(36) Rehr, J. J.; Albers, R. C.; Zabinsky, S. I. *Phys. Rev. Lett.* **1992**, *69*, 3397−3400.
(37) Ravel, B.; Newville, M. *J. Synchrotron Radiat.* **2005**, *12*, 537−541.
(38) Stern, E. A.; Newville, M.; Ravel, B.; Yacoby, Y.; Haskel, D. *Phys. B* **1995**, *208&209*, 117−120.
(39) Ankudinov, A. L.; Ravel, B.; Rehr, J. J.; Conradson, S. D. *Phys. Rev. B* **1998**, *58*, 7565−7576.
(40) Forsellini, E.; Casellato, U.; Tomat, G.; Graziani, R.; Di Bernardo, P. *Acta Crystallogr.* **1984**, *C40*, 795−797.
(41) Sheldrick, G. M. *Acta Crystallogr.* **2008**, *A64*, 112−122.
(42) Hill, C.; Desreux, J. F.; Ekberg, C.; Espartero, A. G.; Galetta, M.; Modolo, G.; Geist, A.; Selucky, P.; Narbutt, J.; Madic, C. *Radiochim. Acta* **2008**, *96*, 259−264.
(43) Bardwell, D. A.; Jeffery, J. C.; Jones, P. L.; McCleverty, J. A.; Psillakis, E.; Reeves, Z.; Ward, M. D. *J. Chem. Soc., Dalton Trans.* **1997**, 2079−2086.
(44) Harthshorn, R. M.; Hey-Hawkins, E.; Kalio, R.; Leigh, G. J. *Pure Appl. Chem.* **2007**, *79*, 1779−1799.
(45) Trumm, S.; Lieser, G.; Panak, P. J. *Radiochim. Acta* **2011**, *99*, 783−790.
(46) Horrocks, W. D.; Sudnick, D. R. *J. Am. Chem. Soc.* **1979**, *101*, 334−340.